

# FLUX ROPE FORMATION PRECEDING CORONAL MASS EJECTION ONSET

L. M. GREEN<sup>1</sup> AND B. KLIEM<sup>1,2,3</sup>

<sup>1</sup>University College London, Mullard Space Science Laboratory, Holmbury St. Mary, Dorking, Surrey, RH5 6NT, UK

<sup>2</sup>Naval Research Laboratory, Space Science Division, Washington, DC 20375, USA and

<sup>3</sup>University of Potsdam, Institute of Physics and Astronomy, Potsdam 14476, Germany

Received 2009 April 27, accepted 2009 June 22

## ABSTRACT

We analyse the evolution of a sigmoidal (S shaped) active region toward eruption, which includes a coronal mass ejection (CME) but leaves part of the filament in place. The X-ray sigmoid is found to trace out three different magnetic topologies in succession: a highly sheared arcade of coronal loops in its long-lived phase, a bald-patch separatrix surface (BPSS) in the hours before the CME, and the first flare loops in its major transient intensity enhancement. The coronal evolution is driven by photospheric changes which involve the convergence and cancellation of flux elements under the sigmoid and filament. The data yield unambiguous evidence for the existence of a BPSS, and hence a flux rope, in the corona prior to the onset of the CME.

*Subject headings:* Sun: coronal mass ejections (CMEs) — Sun: flares — Sun: magnetic fields — Sun: X-rays, gamma rays

## 1. INTRODUCTION

Coronal mass ejections (CMEs) are large scale eruptions of magnetized plasma from the solar atmosphere into the interplanetary space. It is generally accepted that their energy source is derived from the free energy contained in sheared or twisted magnetic fields (Forbes 2000). Many CME models have been developed and despite the differences in the underlying physics of the eruption, all models at some point involve a magnetic flux rope. From this viewpoint, the models can be split into those which require the flux rope to exist prior to the eruption, and those in which the flux rope is formed as a result of topological changes in the course of the eruption.

In the first category the rope is fundamental to the CME initiation process. These models include ideal MHD instabilities of a flux rope (Török & Kliem 2005; Kliem & Török 2006), the force imbalance between a rope and its overlying arcade-like field (Mackay & van Ballegoijen 2006; Bobra et al. 2008), and the catastrophe of the rope-arcade configuration as a whole (Forbes & Isenberg 1991). In the second category, it is proposed that a sheared magnetic arcade becomes unstable to upward expansion (Antiochos et al. 1999; Moore et al. 2001). In the course of the expansion, a vertical current sheet forms in the bottom part of the arcade. Magnetic reconnection in the sheet transforms the inner part of the arcade into a growing flux rope starting early in the expansion process (Lynch et al. 2008) and supporting the expansion in a positive feedback. Obviously, determining whether the pre-eruption magnetic field topology involves a flux rope is key to understanding the physics of CME initiation.

How a flux rope can be formed in the corona prior to an eruption is an open question as well. It may emerge from the convection zone (Rust & Kumar 1994; Low 1996) or be formed in situ by an arcade-to-rope topology transformation (van Ballegoijen & Martens 1989). Numerical simulations of flux emergence indicate that the process essentially stops as the magnetic axis of the rope hits the photosphere, producing a sheared arcade in the corona (Fan 2001). Moreover, pre-CME formation of large-scale flux ropes between active regions and in the quiet Sun cannot occur by emergence.

The theoretical predictions for the evolution of an emerged arcade range from further continuous shearing, keeping the arcade topology until an eruption occurs after 1–2 weeks (van Ballegoijen & Mackay 2007), to the immediate formation of a coronal flux rope, which can find a stable equilibrium or erupt readily, depending on the relative strength and orientation of emerging and preexisting field (Manchester et al. 2004; Archontis & Török 2008). The observations indicate that active regions typically produce eruptions several days after their emergence is largely complete. This is consistent with both, gradual arcade shearing and gradual arcade-to-rope topology transformation (e.g., Amari et al. 2003a,b). Dispersal and diffusion of the photospheric flux concentrations and flows converging toward the polarity inversion line (PIL) of the photospheric field are main drivers of such quasi-static coronal evolution, which often involves flux cancellation in the photosphere along the PIL.

The observational evidence for the existence of a flux rope topology is most compelling for the evolved stage of a CME and gets weaker as earlier phases are considered. Interplanetary data reveal that at 1 AU many CMEs are well described by a flux rope model (Jian et al. 2006) and coronal images often suggest a flux rope topology for erupting filaments and CME cores. Some erupting filaments exhibit a rotation of their axis about the direction of ascent (Rust & LaBonte 2005; Green et al. 2007); this results from a conversion of twist to writhe and implies a flux rope topology. On the other hand, it is unclear whether filaments in their stable equilibrium prior to eruption are contained in fields of flux rope (Rust & Kumar 1994) or arcade topology (Martin 1998) as it is not yet possible to directly measure the three-dimensional structure of the coronal field. Measurements at the photospheric boundary have supported the flux rope topology, however (Lites 2005).

The pre-eruption flux rope formation processes mentioned above involve reconnection at or above the PIL, which, in the case of gradual evolution, is presumably weak and intermittent and in principle not different from the ubiquitous small-scale reconnection events in the solar atmosphere. Therefore, to our knowledge, it has not yet been possible to infer the formation of a flux rope from signatures of reconnection during the quasi-static evolution prior to eruptions. Support

was obtained from the observation of an S shaped emission source at low coronal temperatures, interpreted as cooling plasma on newly reconnected field lines within a flux rope (Tripathi et al. 2009). Events of flux convergence and cancellation at a large-scale PIL presumably represent the clearest indication of the formation process, but are no proof. Another indication, though not a proof either, is the “necking” of coronal cavities in the final stages of their evolution toward eruption (Gibson et al. 2006a). Here we present an investigation of coronal reconnection signatures that demonstrate the formation of a flux rope prior to the onset of a CME.

## 2. BALD-PATCH SEPARATRIX SURFACE

We study a sigmoidal active region (S shaped in X-rays) from the quasi-static evolution, appearing as a long-lived sigmoid, to its eruption, which produced two topologically different stages of a transient sigmoid. Such sources are a signature of locally enhanced dissipation—most likely reconnection, and their occurrence is correlated with CMEs (Canfield et al. 1999). Transient sigmoids are formed in quasi-separatrix layers (QSLs), which represent the interface between two topologically distinct flux systems (Priest & Démoulin 1995); in the case of sigmoids a flux rope and its surrounding arcade (Titov & Démoulin 1999; Green et al. 2007). This may also be true for long-lived sigmoids (Gibson et al. 2006b); alternatively, these may just represent a collection of highly sheared coronal loops, i.e., an arcade (Moore et al. 2001).

The QSL in a flux rope-arcade system can be of two different topologies. It can either intersect itself under the rope along a line of magnetic X-type topology, or extend down to the bottom of the atmosphere (Titov & Démoulin 1999). The latter situation is expected for the emergence of a sub-photospheric flux rope’s full cross section as suggested in Low (1996). Which of the two topologies results from the process of arcade-to-rope transformation, depends upon how high in the atmosphere the reconnection proceeds and whether all reconnected flux under the X line submerges below the photosphere, dragging the X line downward. Both are open questions. We will focus on the topology without an X line, since this is relevant to the data investigated here.

In the absence of an X-type topology under the rope, the QSL touches the PIL tangent to the photosphere, with its field lines pointing in the inverse direction (from the negative to the positive side of the PIL). Sections of the PIL having this property appear as bald patches in  $H\alpha$  images, so the corresponding QSL has become known as bald-patch separatrix surface, BPSS (Gibson & Fan 2006). The field lines passing through bald patches must wrap around the flux rope to connect to their end points on the other side of the PIL (see, e.g., Gibson et al. 2006b, Fig. 3). Hence, they are sigmoidal in shape, being forward (reverse) S for right-handed (left-handed) chirality.

In the process of flux rope formation by arcade-to-rope transformation or by rope emergence, the bald-patch field lines have the highest likelihood of all the field lines in the configuration to be illuminated in X-rays because they pass through the volume of reconnection, at least temporarily. The hot plasma resulting from reconnection expands in the corona along these field lines.

Due to inertial line tying in the photosphere, the bottom of the BPSS must stay largely immobile at coronal timescales. However, the top part of the flux rope can tear apart from the bottom section. This makes the BPSS topology relevant for

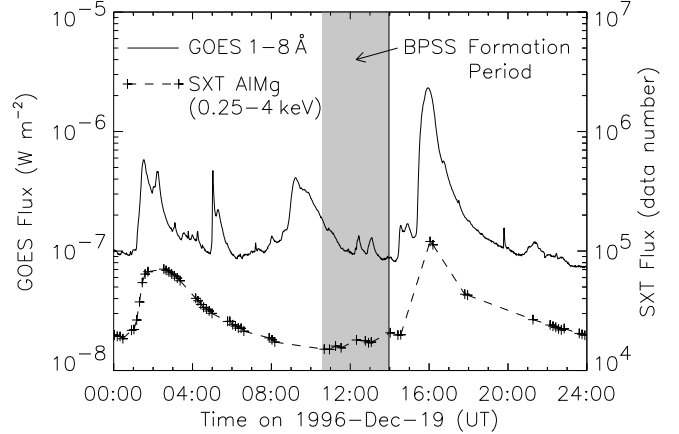


FIG. 1.— Light curves of the flares at 01:22 and 15:21 UT (from GOES and constructed from SXT/AlMg images). The precursors after 14:27 UT also occurred in AR 8005, whereas the flares at 04:57 and 08:23 UT had different locations.

so-called partial eruptions which produce a CME but leave behind filament material in the bottom part of the source volume (Gibson & Fan 2006). In the event of eruption, the bottom part of the BPSS survives and is likely to be illuminated further as the rising upper part of the flux rope tears off, causing a steepening of the currents in the BPSS and, correspondingly, further dissipation. However, a partial flux rope eruption also forms a vertical current sheet above the PIL and inside the original rope, i.e., topologically distinct from the BPSS. Once formed, it becomes the place of strongest energy release, and the flare loops emerging in its downward reconnection outflow are likely to become the brightest X-ray source.

From the above it is clear that a sigmoid can be expected to occur as a signature of flux rope formation in the corona and, reversely, that the observation of a BPSS sigmoid implies a flux rope topology. This sigmoid must be a continuous S crossing the PIL three times, different from a sheared arcade whose loops generally cross the PIL only once. When the flux rope experiences a partial eruption, the middle part of the BPSS sigmoid remains stationary, while a new, brighter X-ray source appears above it, which evolves into the post-eruption arcade.

## 3. SIGMOID AND PHOTOSPHERIC FIELD

NOAA active region (AR) 8005 hosted a forward S sigmoid and produced a CME on 1996 December 19 which was associated with a GOES C2.3 class X-ray flare at 15:21 UT (Figure 1). We study the coronal and photospheric evolution leading to the event using, respectively, half and quarter resolution AlMg and Al.1 filter images recorded by the Soft X-ray Telescope (SXT) onboard *Yohkoh* (Tsuneta et al. 1991) and magnetograms obtained by the Michelson Doppler Imager (MDI) onboard *SOHO* (Scherrer et al. 1995).

The active region was in its decay phase as it rotated over the limb, already having dispersed magnetic polarities and no sunspots. In the three days leading up to the event, the X-ray loops showed a gradual evolution to larger extent, whilst the appearance of a sheared arcade with an overall S shape was maintained (Figure 2). This appearance results from the J shape of the individual loops, produced as a direct consequence of the accumulation of longitudinal flux (pointing along the PIL) in the centre of active regions in the course of their long-term, largely diffusive evolution (van Ballegoijen & Mackay 2007). The dominance of this flux gives all arcade field lines in the middle of the region a

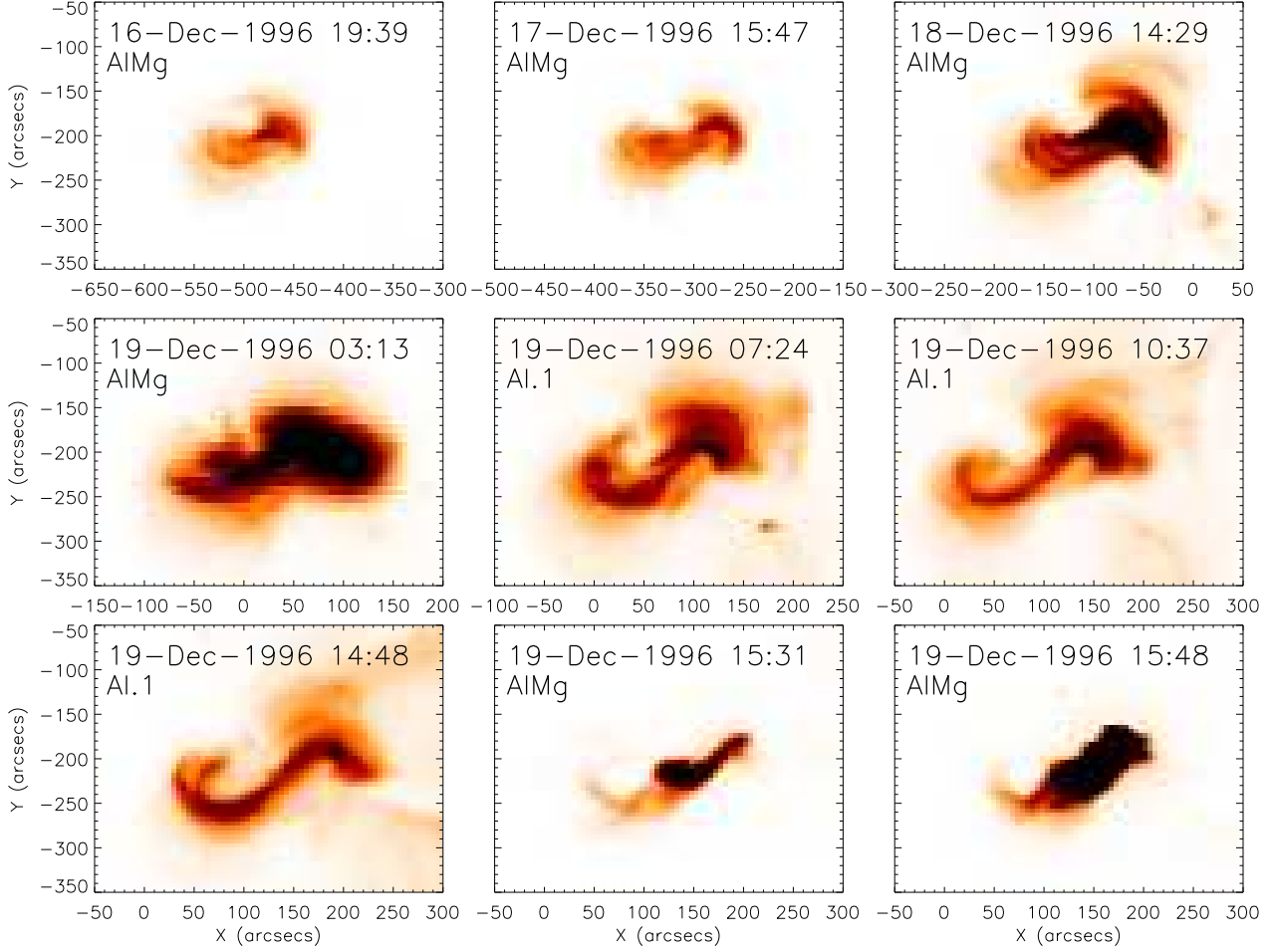


FIG. 2.— SXT images showing the evolution of AR 8005 from a sheared arcade, to point symmetric J shaped loops, to a continuous sigmoid structure, and finally into a sigmoidal flare emission core that grows into the post-eruption arcade.

straight leg and permits them to pass over the PIL only at the edges of the region, producing the J shape.

Beginning at about 00 UT on December 19, the sigmoid narrowed. At 01:22 UT a weak, non-eruptive flare occurred near its northwestern end. After the flare had faded, the sigmoid consisted of two sets of sharper J shaped loops (threads) with shortened straight legs. By 10:37 UT the first J shaped threads had merged into a continuous S, and by the exposure at 13:57 UT the evolution of all visible threads into a continuous S shaped sigmoid was complete (Figure 2). As justified below, we regard this to be a BPSS sigmoid. It had a dip in intensity in its central portion.

The SXT images taken during the main rise of the flare (15:31–15:48 UT) show that the continuous S shaped sigmoid survived the onset of the eruption. Its eastern elbow remained visible under the growing arcade of flare loops for at least two hours, well into the flare decay phase. Moreover, the sigmoid showed no signatures of motion. Its elbows turned around less and shrank somewhat in the course of the flare, but the central part remained stationary. The rise of the soft X-ray flux originated in a new source located in the core of the preexisting sigmoid, overlying its dip. The new source was closely aligned to the preexisting sigmoid’s central section, but with strands seen branching off, so initially it formed a new sigmoid with clearly different end points. It evolved into the post-eruption arcade, which suggests that the new sigmoid was composed

of the first, highly sheared flare loops, formed in the downward reconnection outflow of a vertical current sheet. The evolution of the new sigmoid into the post-eruption arcade was described in greater detail by Sterling et al. (2000), who also concluded that it was a structure different from the pre-existing sigmoid.

H $\alpha$  and Helium 10830 Å data<sup>1</sup> reveal the presence of a filament situated along the PIL, whose central and southeastern section survived the eruption, as seen in the available images at 15:52, 16:57, and 20:33 UT.

The evolution of the photospheric flux was dominated by ongoing dispersal of the main flux concentrations, with no significant emergence of new flux, throughout the disk passage of the active region (see the animated MDI data accompanying Figure 3). This included several episodes in which patches of strong flux detached from the main polarities, approached the PIL, and cancelled. One of these occurred at the northwestern end of the sigmoid between about December 18, 21 UT and December 19, 08 UT and was obviously associated with the small preceding flare. Another, stronger cancellation episode occurred between about December 19, 03 UT and December 20, 11 UT in a narrow region under the middle of the sigmoid, where the two J’s merged into the continuous S (Figure 3). It was preceded by cancellations of weak flux elements

<sup>1</sup> <ftp://nsokp.nso.edu>; <http://www.bbso.njit.edu>

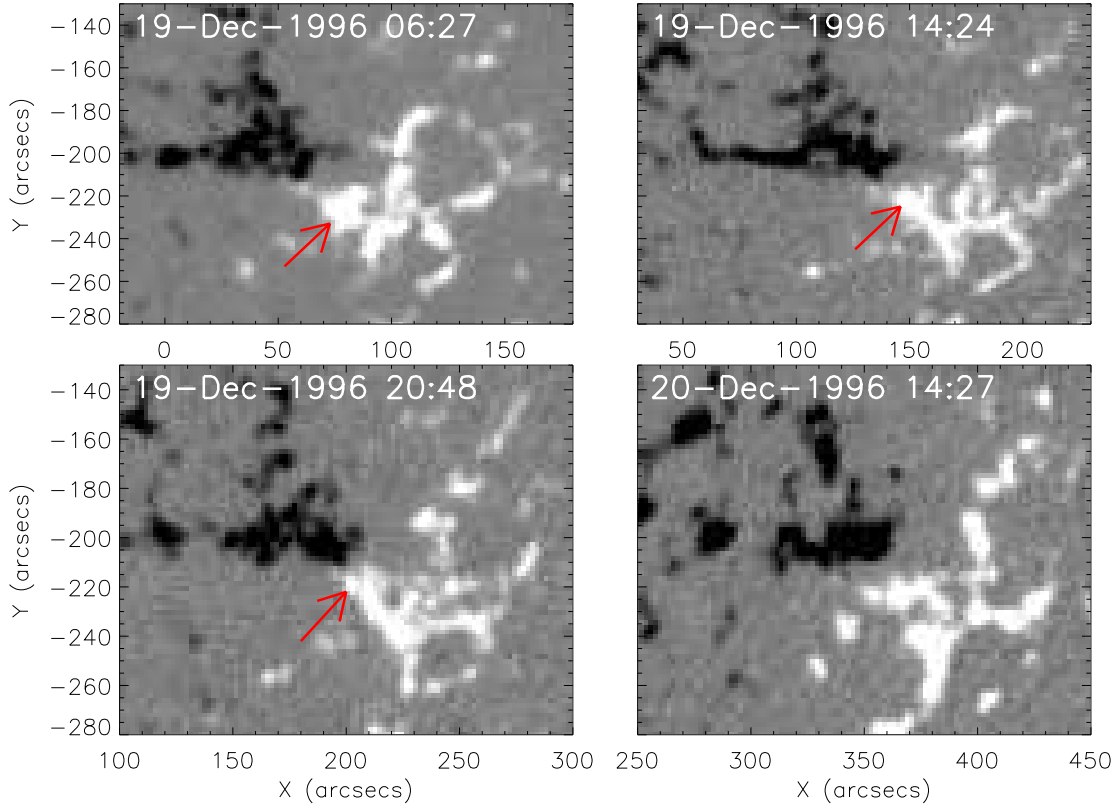


FIG. 3.— MDI magnetogram sequence (saturated at  $\pm 300$  Gauss) showing the flux cancellation episode associated with the formation of the continuous sigmoid. A region of strong positive flux extends and moves toward the PIL (indicated by arrows). When the polarities meet, cancellation occurs and produces a channel of low flux density. An animation of the MDI data throughout December 15–20 is available in the electronic edition of the Journal.

in the same area since about December 18, 20 UT. These data indicate that the changes in the sigmoid were not causally related to the preceding flare, but were driven primarily by the cancellation episode shown in Figure 3.

Co-aligned MDI and SXT data on December 18–19 show that each of the two sets of point symmetric J shaped loops made one crossing of the PIL and had clearly discernible end points at either side of it. When the continuous sigmoid formed, it made three PIL crossings; twice by the sigmoid elbows and once as its central part crossed the PIL in the inverse direction (Figure 4). Overall, the PIL ran at about  $-45^\circ$  inclination to the meridional lines, parallel to the central part of the sigmoid. This is a well known characteristic of sigmoids which so far has prevented the proof of an inverse PIL crossing. However, at the point where the major flux cancellation on December 19–20 occurred and the continuous sigmoid formed, the PIL ran locally nearly east-west, at a substantial inclination to the sigmoid at that point.

#### 4. IMPLICATIONS FOR FLUX ROPE FORMATION

The observations of the sigmoid and the partial eruption of the active region in a CME and flare conform very clearly to the expected signatures of a flux rope with a bald-patch separatrix surface. All key features theoretically predicted were found in the data. These include (1) the formation of a continuous S shaped transient sigmoid from a diffuse, arcade-like long-lived sigmoid, (2) the transient sigmoid’s triple PIL crossing, (3) the co-location of the inverse PIL crossing, the final merging into a continuous S trace, and the area where cancelling strong flux patches converged, (4) the association with a *partial* filament eruption, (5) the transient sigmoid’s survival through the flare peak, and (6) the stationary nature

of its central part during the eruption.

The combination of features 2, 5, and 6 cannot be attained by field lines in an erupting sheared arcade. Partial eruptions and the triple PIL crossing of some field lines within an arcade can be individually arranged in simulations by applying specific photospheric shear profiles (e.g., Antiochos et al. 1994). However, a partial eruption that leaves just the S shaped field lines within the sheared volume in place and essentially stationary is impossible; the sheared flux would always participate in the expansion to some degree. Moreover, the MDI data do not yield any indication of the required shear flow. Consequently, the findings above are conclusive evidence for the formation of a coronal flux rope.

The existence of a BPSS in a long-lived, but eventually erupting, sigmoid was conjectured in another recent case study (McKenzie & Canfield 2008), based primarily on the J shape of the sigmoid threads, which by itself is not conclusive, however (see above). Moreover, only the features 1 and 6 were demonstrated, and no information was given as to whether the transformation from the double-J to the single-S appearance of the sigmoid occurred before or in the course of the eruption.

The formation of the BPSS sigmoid in the active region considered here began over five hours, and was complete over 80 minutes, prior to the onset of the flare. A linear backward extrapolation of the CME height-time data<sup>2</sup> yields an onset time 10 minutes before flare onset. Since the CME was rather fast (with a projected velocity of  $469 \text{ km s}^{-1}$  in spite of its origin near disk centre) and the associated flare was impulsive, it is very unlikely that the CME had a gradual initial evolution

<sup>2</sup> <http://cdaw.gsfc.nasa.gov>



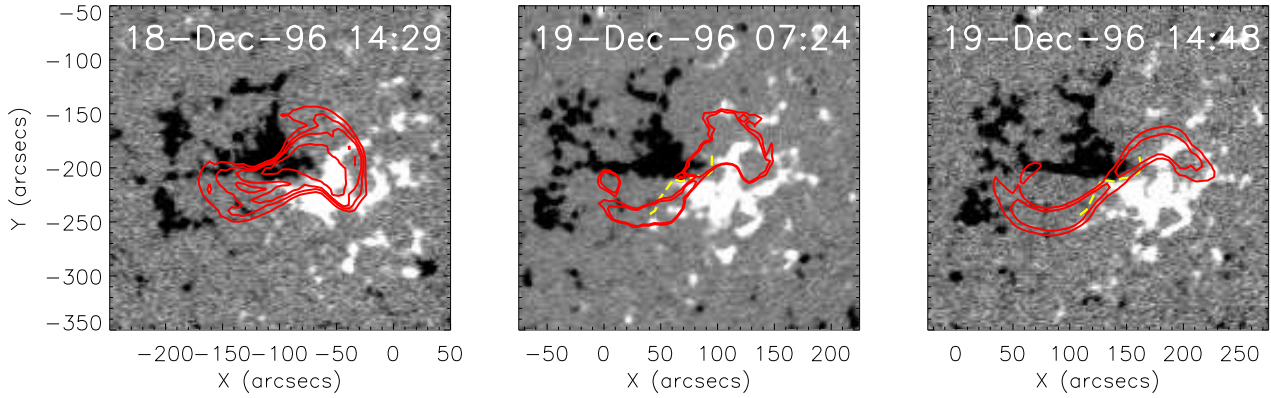


FIG. 4.— Co-aligned MDI and SXT data showing the magnetic connections of the sheared arcade, double-J loops, and continuous sigmoid, and the continuous sigmoid's triple crossing of the PIL (dashed yellow line). The nearest magnetogram in time (saturated at  $\pm 100$  Gauss) was differentially rotated to the time of the SXT data.

with a significantly earlier onset time. Consequently, the data of the sigmoid and eruption imply that a coronal flux rope existed in the active region at least one hour, likely over five hours, *prior* to the onset of the CME.

The data support the gradual arcade-to-rope transformation as the mechanism of flux rope formation because the evolution of the flux was dominated by dispersal and cancellation, not by emergence which had occurred several days earlier.

The transition to the BPSS topology, as seen in soft X-rays, was a process of at least 14 hours in duration. However, the straight legs of the J's did not reconnect with each other immediately, and some of their threads kept a slight separation, albeit decreasing, up to the SXT exposure at 13:10 UT. The question arises of why a continuous S trace wasn't visible throughout the transition. We relate this behaviour to the dominance of the longitudinal flux in the environment of the PIL, mentioned above, which is characteristic of old flux concentrations and clearly indicated for the present active region by the formation of a filament and by the double-J shape of the long-lived sigmoid. Such flux is nearly unidirectional and can hardly reconnect inside when perturbed; essentially it represents a barrier to the approaching flux patches.

Two effects are expected to result in the corona from the observed localised perturbation. Their relative importance depends on the angle between the longitudinal and approaching flux, which controls the strength of reconnection. The approaching flux can slide under the longitudinal flux (which

is rooted remote from the perturbed area), lifting it gradually, as often observed for filaments prior to an eruption. The approaching flux will also reconnect in the interface with the longitudinal flux, illuminating narrow J shaped field line bundles in the interface. As the approach and reconnection progress, the field lines lit up lie closer to the PIL, have one footpoint in the approaching flux, i.e., nearer to the merging point of the sigmoid, and connect to their remote footpoint in an arc at increasing distance (because they were brought in from a more remote location and have to encircle a growing flux rope). These consequences of reconnection are all clearly seen in the SXT data (Figure 2). When the approaching flux eventually reaches direct contact with opposite flux at the PIL beneath existing longitudinal flux (as indicated by the continued presence of the filament), the shortened straight legs of the J's merge into a continuous S by reconnecting with each other near their end points. The flux they were temporarily rooted in submerges in the cancellation event, leaving a flux rope with BPSS topology.

We acknowledge the use of data provided by the Global High Resolution  $H\alpha$  Network, the *Yohkoh*/SXT, *SOHO*/MDI, and *GOES* instruments, and by the CME catalog held at NASA's CDAW Data Center. This work was supported by The Royal Society, STFC, NSF grant ATM 0518218, and NASA grant NNN06AD581.

#### REFERENCES

- Amari, T., Luciani, J. F., Aly, J. J., Mikic, Z., & Linker, J. 2003a, *ApJ*, 585, 1073  
 Amari, T., Luciani, J. F., Aly, J. J., Mikic, Z., & Linker, J. 2003b, *ApJ*, 595, 1231  
 Antiochos, S. K., Dahlburg, R. B., & Klimchuk, J. A. 1994, *ApJ*, 420, L41  
 Antiochos, S. K., DeVore, C. R., & Klimchuk, J. A. 1999, *ApJ*, 510, 485  
 Archontis, V., & Török, T. 2008, *A&A*, 492, L35  
 Bobra, M. G., van Ballegoijen, A. A., & DeLuca, E. E. 2008, *ApJ*, 672, 1209  
 Canfield, R. C., Hudson, H. S., & McKenzie, D. E. 1999, *Geophys. Res. Lett.*, 26, 627  
 Fan, Y. 2001, *ApJ*, 544, 111  
 Forbes, T. G. 2000, *J. Geophys. Res.*, 105, 23153  
 Forbes, T. G., & Isenberg, P. A. 1991, *ApJ*, 373, 294  
 Gibson, S. E., & Fan, Y. 2006, *ApJ*, 637, L65  
 Gibson, S. E., Fan, Y., Török, T., & Kliem, B. 2006b, *Space Sci. Rev.*, 124, 131  
 Gibson, S. E., Foster, D., Burkepile, J., de Toma, G., & Stanger, A. 2006a, *ApJ*, 641, 590  
 Green, L. M., Kliem, B., Török, T., van Driel-Gesztelyi, L., & Attrill, G. D. R. 2007, *Sol. Phys.*, 246, 365  
 Jian, L., Russell, C. T., Luhmann, J. G., & Skoug, R. M. 2006, *Sol. Phys.*, 239, 393  
 Kliem, B., & Török, T. 2006, *Phys. Rev. Lett.*, 96, 255002  
 Lites, B. W. 2005, *ApJ*, 622, 1275  
 Low, B. C. 1996, *Sol. Phys.*, 167, 217  
 Lynch, B. J., Antiochos, S. K., DeVore, C. R., Luhmann, J. G., & Zurbuchen, T. H. 2008, *ApJ*, 683, 1192  
 Mackay, D. H., & van Ballegoijen, A. A. 2006, *ApJ*, 641, 577  
 Manchester, W. IV, Gombosi, T., DeZeeuw, D., & Fan, Y. 2004, *ApJ*, 610, 588  
 Martin, S. F. 1998, *Sol. Phys.*, 182, 107  
 McKenzie, D. E., & Canfield, R. C. 2008, *A&A*, 481, L65  
 Moore, R. L., Sterling, A. C., Hudson, H. S., & Lemen, J. R. 2001, *ApJ*, 552, 833  
 Priest, E. R., & Démoulin, P. 1995, *J. Geophys. Res.*, 100, 23 443  
 Rust, D. M., & Kumar, A. 1994, *Sol. Phys.*, 155, 69  
 Rust, D. M., & LaBonte, B. J. 2005, *ApJ*, 622, L69  
 Scherrer, P. H., et al. 1995, *Sol. Phys.*, 162, 129  
 Sterling, A. C., Hudson, H. S., Thompson, B. J., & Zarro, D. M. 2000, *ApJ*, 532, 628

- Titov, V. S., & Démoulin, P. 1999, A&A, 351, 707
- Török, T., & Kliem, B. 2005, ApJ, 630, L97
- Tsuneta, S., et al. 1991, Sol. Phys., 136, 37
- Tripathi, D., Kliem, B., Mason, H. E., Young, P. R., & Green, L. M. 2009, ApJ, 698, L27
- van Ballegoijen, A. A., & Mackay, D. H. 2007, ApJ, 659, 1713
- van Ballegoijen, A. A., & Martens, P. C. H. 1989, ApJ, 343, 971